Optimization of the design of a wall-less Hall thruster

IEPC-2015-182／ISTS-2015-b-182

Presented at Joint Conference of 30th International Symposium on Space Technology and Science
34th International Electric Propulsion Conference and 6th Nano-satellite Symposium,
Hyogo-Kobe, Japan
July 4 – 10, 2015

S. Mazouffre[1], J. Vaudolon[2], and S. Tsikata[3]
CNRS, ICARE, 1c Avenue de la Recherche Scientifique, 45071, Orléans, France.

and

C. Hénaux[4], D. Harribey[5], and A. Rossi[6]
Laboratoire Plasma et Conversion d'Energie, Université de Toulouse, UPS, INPT Toulouse,
2 rue Charles Camichel, F-31071 Toulouse cedex 7, France.

Abstract: An alternative Hall thruster architecture that shifts the ionization and acceleration regions outside the cavity has recently been developed in our team. This unconventional design has been termed a Wall-Less Hall Thruster. Such a device could offer significant benefits in terms of integration, operating envelope and lifetime, since the plasma interaction with the walls are significantly reduced. A 200 W-class prototype with permanent magnets has been developed and tested to demonstrate the validity of this new concept. Preliminary experiments with a simple design have shown the magnetized discharge is stable when the electric field is shifted outside the cavity. Moreover, the ion production and acceleration processes are not disturbed in wall-less configuration. However, experiments have also revealed that moving the anode to the exit plane without any other changes leads to a large discharge current and low overall performances. In this contribution, we present recent experimental results about an optimized version of the wall-less Hall thruster concept. Studied have been performed with the 1.5 kW PPS-Flex Hall thruster as it offers a unique magnetic field flexibility. The anode geometry and the magnetic field topology have been modified to avoid interaction between the magnetic field lines and the anode surface. Thrust and discharge current have been measured over a broad range of xenon propellant mass flow rates and applied voltages. Outcomes indicate the current is strongly reduced and a high thrust efficiency, similar to the standard case, is achieved with an optimized wall-less configuration.

Nomenclature

B	=	Magnetic field (G)	T	=	Thrust (mN)
E	=	Electric field (V/m)	U_d	=	Applied voltage (V)
η	=	Anode efficiency	V_b	=	Ion beam energy (eV)
Φ_a	=	Anode gas mass flow rate (mg/s)	v_d	=	Electron drift velocity (m/s)
I_d	=	Discharge current (A)	x	=	Axial position (m)

[1] CNRS research scientist, head of the Electric Propulsion team; stephane.mazouffre@cnrs-orleans.fr
[2] PhD candidate, EP team; julien.vaudolon@cnrs-orleans.fr
[3] CNRS research scientist, EP team; sedina.tsikata@cnrs-orleans.fr
[4] Associate Professor, Insitut National Polytechnique de Toulouse; carole.henaux@laplace.univ-tlse.fr.
[5] Engineer at CNRS, INP Toulouse; dominique.harribey@laplace.univ-tlse.fr
[6] Ph.D. candidate, INP Toulouse; alberto.rossi@laplace.univ-tlse.fr

I. Introduction

THE change from chemical to electrical propulsion systems permits a drastic reduction in propellant mass, as illustrated by the well-known Tsiolkovsky rocket equation. This mass reduction translates into important cost-savings for the satellite operator. Hall thrusters (HTs) are advanced and mature electrical propulsion devices dedicated to space applications.[1,2] They are currently used for station-keeping and attitude control of geosynchronous communication satellites. In the very near future, high-power Hall thrusters will also be used for high delta-v maneuvers like orbit topping and orbit transfer maneuvers, making "all-electric" satellite platforms a reality. Hall thrusters are efficient gridless ion accelerators. Their operating principle relies on the creation of a low-pressure quasi-neutral plasma discharge in a crossed magnetic and electric field configuration, in which a propellant gas, typically xenon, is ionized and accelerated.[3,4] In the standard configuration, the magnetized discharge is confined to an annular dielectric cavity with the anode at one end, where the gas is injected, and an external cathode that also serves as beam neutralizer. Ionization of the propellant gas occurs inside the cavity. Subsequently, ions are accelerated through a potential drop that stretches from the interior to the exterior of the cavity. Compared to traditional gridded ion engines, Hall thrusters produce a moderate specific impulse but they furnish a large thrust-to-power ratio. The main drawback of conventional HTs is the fact that the wall material determines to a large extent the discharge properties, and consequently, the performance level, as well as the operational lifetime. The wall material plays a role in the plasma properties, through, among other effects, secondary electron emission. The primary factor that limits the lifetime is the erosion of the dielectric annular channel walls due to bombardment by hot electrons and high-energy ions.[5,6] In addition, plasma-wall interaction generates power losses and thermal stress on the structure components. The large particle flux towards the walls is a direct consequence of the magnetic field topology. In a HT, the accelerating electric field originates in a decrease of the electron mobility at the channel exit. An efficient barrier requires a radial magnetic field, the lines of which intersect the walls. Recently, an original approach to significantly reducing the erosion rate, hence prolonging the thruster lifetime, has been proposed and validated. This approach is termed magnetic shielding (MS).[7-12] MS consists of preventing the magnetic field lines from crossing the walls in the acceleration region. Instead, the lines remain parallel to the wall of the downstream section of the channel and they extend to the anode region to capture cold electrons. Such a topology strongly reduces the magnitude of the radial electric field component, thereby decreasing wall material sputtering.

There is another, more drastic, alternative to limit interactions between the plasma and the surface in a HT. The principle is to shift the ionization and acceleration regions outside the cavity. This unconventional design was named a Wall-Less Hall Thruster, or WL-HT in short.[13,14] In a WL thruster, the anode is moved to the exit plane of the dielectric channel. As shown in a recent work, the electric field is then entirely shifted outside the cavity, in a region where the magnetic field gradient is negative. Note that a WL Hall thruster differs from a Thruster with Anode Layer. In the latter, a guard ring placed at the anode exit plane is maintained at the external cathode potential to avoid a potential drop outside the cavity. As a consequence, the electric field is created in the vicinity of the exit plane. On the contrary, in the WL concept the electric field location is not forced but it results from the plasma properties downstream the cavity exhaust. Preliminary characterization of a low-power permanent magnet wall-less Hall thruster prototype and experiments with laser spectroscopy and electrostatic probes have shown the plasma discharge is stable in WL configuration. However, the discharge current collected by the anode is very large and the performance level is low if the anode geometry and **B** field topology are not modified.

In this contribution, we present recent experimental results about an optimized version of the wall-less Hall thruster concept. Studied and experimental campaigns have been performed with the 1.5 kW-class PPS-Flex Hall thruster as it offers a unique magnetic field flexibility.[15,16] The anode geometry and the magnetic field topology have been modified to limit interaction between the magnetic field lines and the anode surface. Thrust and discharge current have been measured over a broad range of xenon propellant mass flow rates and applied voltages. Outcomes of test sequences and characterizations indicate the current is strongly reduced and a relatively high thrust efficiency is achieved with an optimized wall-less configuration.

II. Proof-of-concept

A. Design of the first WLHT prototype

The standard configuration of a Hall thruster is schematically depicted in Figure 1. Details can be found in references.[2-4] An anode is placed at the back of an annular ceramic channel. In many designs the anode is also used as a gas injector. The cathode, which produces the electron current for discharge balance and ion beam neutralization, is located outside the channel. Permanent magnets or coils are used to generate a radially directed magnetic field with a bell-shaped intensity distribution along the channel axis. Typically, the peak amplitude of the

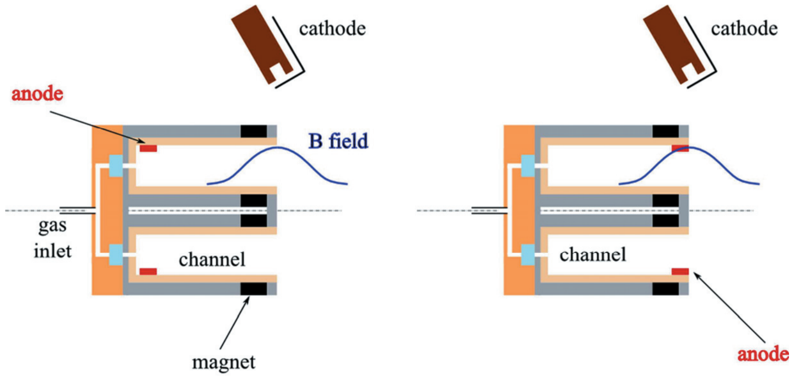

Figure 1. (Left) Layout of the configuration of a standard single-stage Hall thruster. The anode is placed at the back of a ceramic channel. The magnetic field strength is maximum at the channel exit plane. (Right) Basic transformation into a wall-less HT. The anode is shifted towards the channel exit plane. The other elements (**B** field, geometry, wall material, cathode) stay unchanged.

magnetic field is reached at the channel exit plane, as illustrated in Figure 1. The dielectric channel confines the neutral gas, therefore maintaining a relatively high atom density necessary for an efficient ionization process, as well as the created plasma. To shift both the ionization and the acceleration regions outside the thruster cavity, the simplest way is to move the anode towards the channel exit plane, as illustrated in Figure 1, without modifying anything else. The shape and sizes stay unchanged, like the cavity material and the magnetic field topology. This is the basic method for transforming a HT into a WL-HT, however, optimization of the thruster in its new configuration in fact requires other changes, as we shall see in the next chapter.

The first prototype was based on the PPI thruster architecture.[17,18] The PPI thruster is a 200W-class Hall thruster which delivers a thrust of 10 mN when operated at 250 V and 1.0 mg/s xenon mass flow rate. In the study dedicated to the proof-of-concept, the channel dielectric walls were made of BN-SiO_2. The channel was in the $2S_0$ configuration, meaning that the width-to-mean diameter ratio was twice the standard ratio,[17] the latter of which is defined as that of the well-known Russian SPT100 thruster. The anode used for the first prototype was a 5 mm wide stainless steel ring. It was wound around the external wall at the channel exit plane, where the **B** field amplitude is the highest. Xenon is used as a propellant gas. A heated hollow cathode with a LaB_6 insert was used with a constant mass flow rate of 0.2 mg/s. The cathode orifice was placed 10 cm below the thruster symmetry axis and 3 cm away from the channel exit plane.

Figure 2 shows a set of photographs of the low-power PPI thruster firing with Xe in the NExET vacuum chamber in standard configuration and in wall-less configuration with a ring anode. Pictures were taken with the same camera settings. The operating conditions were: U_d = 200 V with a gas mass flow rate of 1 mg/s. The background gas pressure inside the tank was 3.5×10^{-5} mbar-Xe. The plasma discharge is moved outside the dielectric cavity in wall-less configuration, as illustrated by the strong light intensity in front of the exit plane. It is also interesting to note the ion beam boundaries are less sharp in WL. For instance, the light of the on-axis structure that originates in the interaction of elementary beams from opposite sides of the channel is faint. It certainly indicates a larger ion beam divergence in WL as well as a low level of performance.

B. Electric field distribution

The time-averaged distribution function of the axial velocity component of metastable Xe^+ ions was measured along the channel axis of the Hall thruster by means of Laser Induced Fuorescence (LIF) spectroscopy at 834.72 nm for the two configurations. Details of the experimental arrangement and the LIF technique and optical bench can be found elsewhere.[19,20] In Figure 3(left), the most probable ion velocity, i.e., the velocity for which the VDF is the highest, is plotted as a function of the position x along the channel axis for a discharge voltage of 200 V and a Xe gas flow rate of 1 mg/s. The position x = 0 refers to the channel exit plane. With a standard design, the ion acceleration process starts upstream of the exit plane. At x = 0 mm, the ion velocity is already 5200 m/s. Beyond the exit plane, the velocity increases over a short distance of about 20 mm and attains a maximum of 15200 m/s. With the wall-less prototype, the acceleration region is entirely shifted outside the channel. The velocity is typically

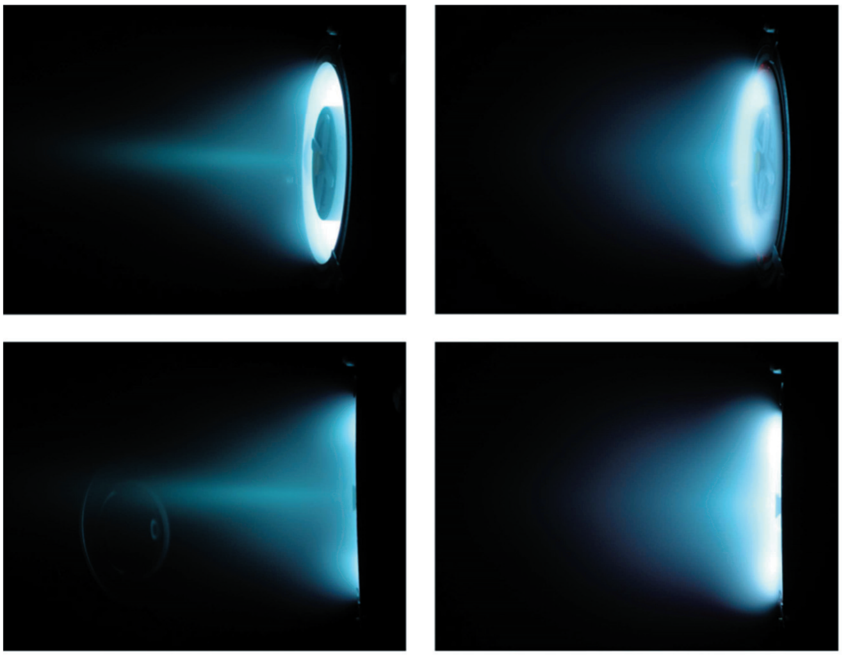

Figure 2. (Left) Photographs of the low-power PPI Hall thruster firing with Xe at 200 V and 1 mg/s in standard configuration. (Right) Photographs of the first WL-HT prototype firing with Xe under identical conditions. In the latter case the anode is a conducting ring located at the channel exit plane around the external wall. The **B** field topology stayed unchanged.

150 m/s inside the channel. This value is close to the thermal speed for xenon atoms at 300 K, but below the atom velocity at the channel exhaust, which is typically 500 m/s in the standard configuration due to ion recombination at walls.[19,21] The very low ion axial velocity inside the cavity of a WL-HT source is therefore an indirect proof that plasma-surface interaction has been reduced. The maximum velocity is 13510 m/s.

The accelerating potential, also called the beam energy V_b, corresponds to the potential drop experienced by the ions. It is directly computed from the velocity. In the standard configuration, V_b is 160 eV, whereas it is only 120 eV in the WLHT. The low final ion axial velocity, i.e., the low beam energy, in WL configuration indicates a poor energy conversion efficiency in the axial direction. Energy losses may originate in the strong curvature of the magnetic field lines in the acceleration region, which makes the ion beam diverge, as suggested by Fig. 2.

In steady-state conditions, the accelerating electric field profile can be directly inferred from the profile of the ion velocity axial component using the energy conservation equation.[20] The electric field distribution along the channel axis of the WL-HT is shown in Fig. 3(right) for 200 V and 1 mg/s. The electric field profile measured in the conventional configuration is also shown in Fig. 3b for comparison. As expected, the electric field is situated outside the cavity in the WL-HT. The length of the acceleration region is about 15 mm, similar to the size observed with the standard configuration. The shift of the electric field towards the exterior has been observed by LIF for other experimental parameters: 150 V and 0.8 mg/s and 85 V and 1.3 mg/s.[14] Emissive probe measurements also confirmed the outward shift of the **E** field as well as PIC numerical simulations[22]. In Fig. 3, the electric field is shifted 10 mm outside the cavity in WL mode. The distance is then larger than the channel width. Surprisingly, it appears that the electron drift velocity $v_d = E_x/B_y$, which plays a fundamental role in turbulent electron diffusion through the magnetic barrier[23-25], stays unchanged when modifying the design. The drift velocity is 9×10^5 m/s, respectively 7.5×10^5 m/s, in standard, respectively wall-less, configuration. The difference between the two values is within the measurement error margin.

C. Current-voltage characteristics

The discharge current waveform measured on the anode line for several operating parameters, along with the associated power spectrum, was presented and discussed in a preceding study.[13] In short, the current time series is not much affected by a change from a standard configuration to a WL mode. The breathing oscillation is observed in

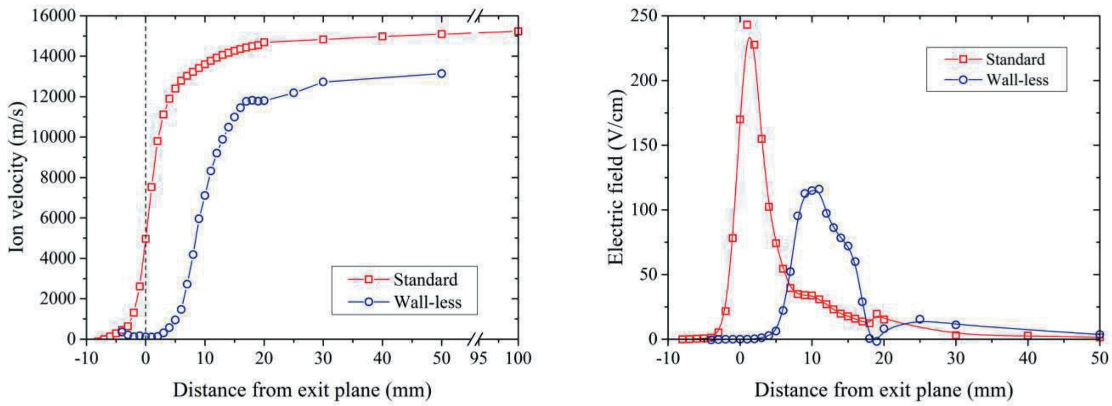

Figure 3. Left) Most probable Xe^+ ion velocity along the channel axis of the ion source. Right) Corresponding accelerating electric field distribution. Standard (square) and WL-HT (circle) configurations. The conditions were 200 V and 1 mg/s.

WL mode with unaffected frequency band and intensity. The fact that the breathing mode is not influenced by the thruster design indicates the main physical processes that govern ionization in the HT cross-field discharge remain unchanged. Oscillations around 100 kHz are observed in the standard configuration but they are absent, or at least much weaker, in WLHT whatever the operating conditions. These oscillatory phenomena encompass phenomena such as rotating instabilities and ion transit time instabilities.

The graph in Fig. 4 shows the anode discharge current as a function of the applied voltage for various xenon gas mass flow rates. The current-mass flow rate envelope is similar for the two configurations, i.e., the thruster can operate with the same parameters. However, the discharge current is higher in the case of the WL-HT whatever the voltage-flow rate couple. The difference increases with the gas flow rate and the applied voltage. Moreover, the rate of change of I_d with U_d is positive in WL, whereas it is negative in standard mode for most flow rates. As the maximum input power is allowed to exceed 300 W only for a short time to prevent damage to the device, the WL mode is limited in voltage at large mass flow rate. As can be seen in Fig. 5, at 200 V, the current increases from 1.34 A to 2.21 A when the configuration is switched from a standard to a WL-HT mode (an increase of 64%). Such

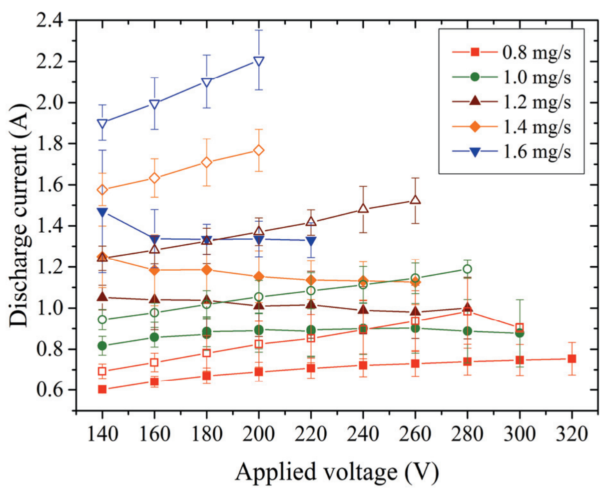

Figure 4. Anode discharge current against applied discharge voltage for several xenon mass flow rates in the standard (full symbols) and WL-HT (open symbols) configurations. Error bars indicate the current standard deviation.

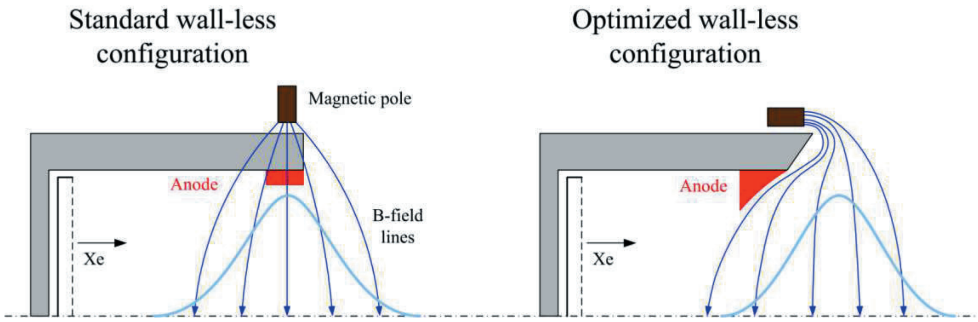

Figure 5. Left) Basic configuration of a wall-less Hall thruster: The anode is simply moved at the channel exit plane. The magnetic field lines intercept the anode. Right) Optimized wall-less design: The magnetic field lines are parallel to the anode.

an increase cannot be attributed to an improved gas ionization. The large discharge current in the WL mode is due to a larger diffusion of the electrons, in other words a less efficient electron confinement, in the region of strong magnetic field. With the non-optimized WL-HT thruster design, see Fig. 1, the electron resistivity is reduced in front of the thruster. With a classical topology, magnetic field lines are perpendicular to the walls at the channel exhaust. Therefore many magnetic field lines intersect the anode in WL mode, making the passage of hot electrons coming from the outside plasma to the anode easier. The fact that electrons cannot transfer a large fraction of their energy to the gas in this WL design implies a lower ionization degree.

Figure 5 also shows that the discharge current standard deviation is not greatly affected when the anode is moved towards the channel exit plane. That confirms the oscillation level of the breathing mode does not depend on the configuration. This fact reveals that, overall, the ionization and acceleration mechanisms do not change, or, in other words, the underlying physics remains unchanged at the macroscopic level.

In summary, the discharge can be ignited and it is stable in wall-less configuration. The electric field profile and the ionization zone are shifted outwards the channel, as expected. The electric field exists in a region with no physical boundary in the radial direction and where the magnetic field gradient is negative. The interaction between high energy ions and ceramic surfaces is therefore negligible in a WL Hall thruster. This aspect is obviously of great relevance for allowing high-voltage operation and for prolonging the lifetime of the device. Moreover, the low-frequency oscillations of the discharge current I_d(t) are not modified in a WL configuration, which warrants the physical mechanisms at the origin of the thrust are preserved.

However, measurements show the discharge current is much higher in WL mode. The thermal load experienced by the thruster is also large and the beam energy is low. The efficiency of the device is therefore low. The first low-power thruster prototype was intended for demonstrating the validity of the Wall-Less concept and for obtaining some insights into the discharge and ion beam properties. Although the WLHT concept has proven to be valid, experimental outcomes nevertheless reveal that the WL concept must be optimized in order to reach an acceptable performance level.

III. Optimization of the wall-less design

A. Anode geometry and magnetic field topology

Figure 5(left) illustrates the interaction between the anode and the magnetic field lines in the basic configuration of the first WL Hall thruster prototype. As previously explained, the **B**-field lines are perpendicular to the thruster axis with a standard magnetic topology and they intercept the anode that is placed at the channel exhaust. The magnetic confinement therefore becomes much less efficient. A large fraction of hot electrons originating from the external cathode and trapped along **B**-field lines are directly lost at the anode. The discharge current is therefore high and the ionization degree decreases.

In order to prevent electron losses at the anode, the magnetic barrier must be restored. The basic idea is to make the magnetic field lines parallel to the anode surface. The anode could be rotated at 90° without changing the magnetic topology. This design is, however, not efficient for two reasons, namely: i) a large fraction of the magnetic

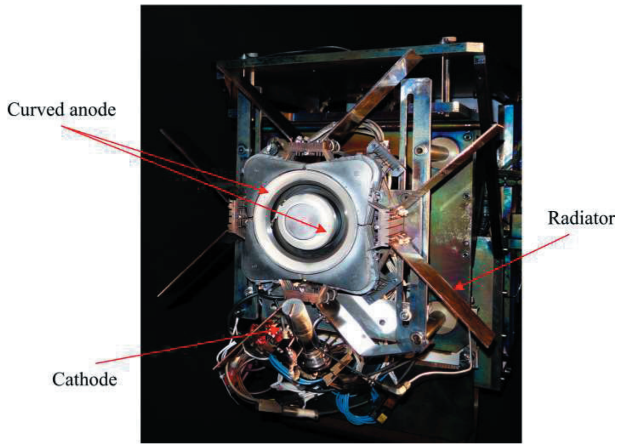

Figure 6. Photograph of the PPS-Flex Hall thruster in WL configuration mounted onto the thrust balance of the PIVOINE-2g test bench.

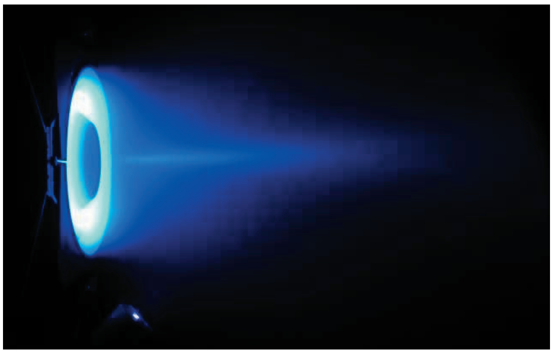

Figure 7. Photograph of the PPS-Flex Hall thruster in WL configuration operating with xenon ($U_d = 350$ V, $\Phi_a = 2.5$ mg/s).

flux is injected into the channel and it does not play any role in the electron trapping and thrust production and ii) the magnetized region, where ionization and acceleration take place, is short, i.e. the number of electron-atom collision events is rather low. Figure 5(right) exemplifies a more suitable design. The magnetic barrier is located in front of the channel exit plane by injecting the magnetic flux in the *x* direction. The maximum of the **B**-field magnitude is then shifted outside the cavity. The anode is still placed at the channel exhaust, but its shape is curved to avoid any interaction with the magnetic field lines: The lines never cross the anode surface. The optimized WL magnetic topology resembles the magnetic shielding (MS) topology.[7-11] There is nevertheless one main difference. The magnetic field lines do not have to extend deep into the channel to capture cold electron. This difference makes easier the generation of a WL topology by means of a magnetic circuit compared to a MS topology.

B. Experimental campaigns with the PPS-Flex Hall thruster

The optimization of a WLHT has been investigated with the PPS-Flex Hall thruster.[15,16] The PPS-Flex thruster is a 1.5 kW-class Hall thruster based on the Snecma PPS®1350 thruster architecture. It is a unique prototype in terms of magnetic flexibility. Compared with a classical magnetic circuit, the circuit of the PPS-Flex has been especially designed to control in an independent manner all the characteristic parameters of a magnetic topology. The PPS-Flex is composed of 22 coils: 4 internal coils; 4 external stages, each with 4 coils connected in series, and two back coils. The PPS-Flex operation therefore requires independently controlling ten power supplies for the **B** field generation. Experiments have been performed with the second version of the PPS-Flex thruster. This new version is equipped with additional heat pipes and with 8 large external radiators to reach a high input power level without damaging the magnetizing coils and the circuit. The thruster has been fired up to 2 kW without troubles. Figure 6 shows a photograph of the PPS-Flex Hall thruster in WL configuration mounted on the thrust stand of the PIVOINE-2g test bench in Orléans.

In WL configuration, the PPS-Flex has been equipped with a curved anode split in two parts, as can be seen in Fig. 6. The inner and outer rings are located at the exit plane of the straight section of the BN-SiO_2 channel and connected to one another. Note that the straight cavity corresponds to the cavity of the PPS®1350 thruster. The conical section is used to protect the last magnetic stage.[15] The magnetic field topology has been changed and optimized during the experiments. The typical topology is given in Fig. 5. Two experimental campaigns were performed. The optimization procedure was first tested at the ESA Propulsion Laboratory (ESA-ESTEC) in the Netherlands in October 2014. The PPS-Flex in WL mode was fired in the CORONA vacuum chamber. Preliminary testing validated the optimization approach for the **B**-field topology. The discharge could be ignited without trouble. Moreover, the discharge current drastically decreased when switching from a standard magnetic map to a WL map, as expected. A second campaign was conducted at ICARE in the PIVOINE-2g vacuum chamber in April 2015. The anode geometry and the magnetic map have been further optimized to reach a high thrust efficiency. Several quantities have been acquired: the thrust, the discharge current time series, the ion current density profile with a Faraday cup and the thruster component temperature by means of calibrated infrared thermal imaging.[26,27] During this campaign, the thruster was operated over of broad range of parameters: U_d = [200 – 500] V,

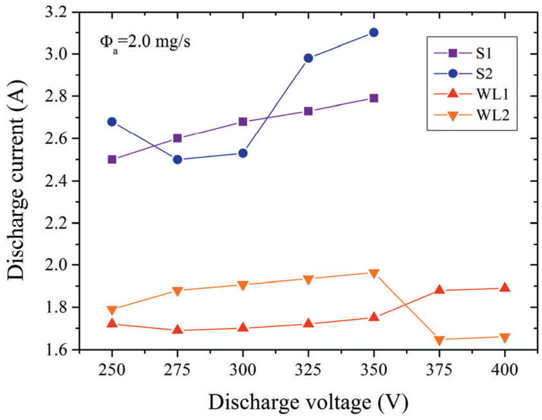

Figure 8. Current-voltage plots in standard (S) and wall-less (WL) configuration obtained with the PPS-Flex ($\Phi_a = 2$ mg/s).

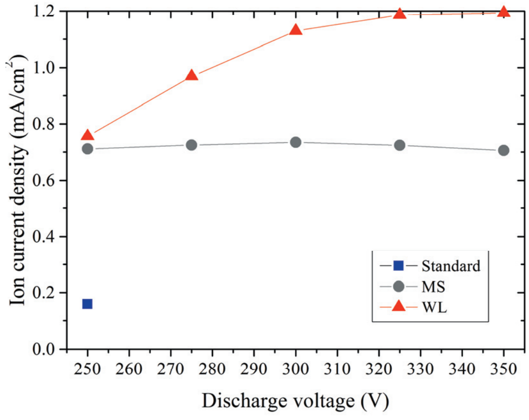

Figure 9. On-axis ion current density against discharge voltage in standard, magnetic shielding (MS) and wall-less (WL) modes (PPS-Flex, $\Phi_a = 3.5$ mg/s).

Φ_a = [2 – 3.5] mg/s, power = [400 – 1500] W. A heated hollow cathode with a LaB_6 insert was used with a constant mass flow rate of 0.4 mg/s during the two campaigns. The cathode and the thruster body were floating but unbound. A picture of the PPS-Flex thruster in WL configuration firing with Xe in the PIVOINE-2g chamber is displayed in Fig. 7. This photograph must be compared with the picture of the first WL prototype displayed in Fig. 2(right). When optimizing the design, the contrast ratio is high, boundaries are sharp and the plume structure is well-defined, as it is the case with a high-efficiency Hall thruster. The discharge is bright inside the conical channel and a spike of plasma extends far downstream along the channel centerline. The plume is in the so-called "spike mode" in Fig. 7.

C. Current and thrust measurements

The discharge current was measured as a function of the applied voltage for several magnetic field topologies. Figure 8 illustrates the results obtained at the EPL with the PPS-Flex. The anode geometry was not optimized in this case. As can been seen, the current decreases drastically when switching from a standard-like to a wall-less-like magnetic topology. A similar trend was observed with larger xenon anode mass flow rates.

During the campaign at EPL, the ion current density was measured by means of a Faraday cup on the thruster centerline. Results are shown in Fig. 9 for several applied voltages and for 3 magnetic topologies with $\Phi_a = 3.5$ mg/s. Here MS refers to a Magnetic Shielding type topology. With the anode placed at the exit plane, the ion current density is the highest for a WL magnetic configuration whatever the voltage. The on-axis value reaches ~ 1 mA/cm^2 at 300 V, which is typical for a well-designed Hall thruster.

The experimental outcomes therefore confirm i) the increase in discharge current observed with the first prototype is due to the electron fluid, ii) the magnetic confinement can be restored with a well-defined **B** field topology and iii) the ion current can be large with an optimized magnetic field map for a WL configuration.

The thrust level has been measured in the PIVOINE-2g test-bench. Both the anode geometry and the magnetic field topology were optimized for these experiments, see previous section. Data analysis is still ongoing but some first results are presented in Tab. 1 for various xenon mass flow rates and applied voltages. The anode efficiency is computed using the following formula:

$$\eta = \frac{T^2}{2\Phi_a U_d I_d}. \qquad (1)$$

Table 1. Discharge current, input power, thrust level, anode efficiency and specific impulse determined for the PPS-Flex Hall thruster in optimized wall-less configuration for various operating conditions.

Anode mass flow rate	Discharge voltage	Discharge current	Power	Thrust	Anode Efficiency	Specific impulse
[mg/s]	[V]	[A]	[W]	[mN]	#	[s]
3.0	300	2.8	820	39.0	0.32	1359
	380	3.9	1485	44.8	0.23	1561
2.5	200	2.0	404	24.8	0.31	1035
	400	2.6	1052	36.5	0.26	1520
2.0	200	1.5	297	17.3	0.26	911
	400	2.0	775	28.2	0.26	1483
	500	2.4	1170	28.9	0.18	1516

The specific impulse is given by:

$$Isp = \frac{T}{g_0 \Phi_a}, \qquad (2)$$

where g_0 is the gravity of Earth at sea level. As can be seen in Tab. 1, the discharge current intensity is low and in agreement with the injected mass flow rate, and the thrust level, the specific impulse and the anode efficiency reach acceptable values for relatively low mass flow rates. The quantities are in fact not far from standard values for a high-efficiency 1.5 kW-class Hall thruster. The gap can be explained by the fact that the maximum magnitude of the **B** field was only 70 G, which limits the electron confinement. The low magnetic field strength in MS and WL configuration originates from the actual design of the PPS-Flex thruster magnetic circuit. The original PPS-Flex prototype has not been considered for generating efficient MS- and WL-type magnetic topologies. Therefore a third version of the PPS-Flex thruster able to provide a high **B** field magnitude whatever the topology is currently under development.

Notice the thruster was operated up to 500 V. In addition, the stability of the discharge has been verified by operating the thruster in optimized WL mode at 300 V and 3.0 mg/s during 1 hour. The discharge current reached a steady state at 2.75 A with a standard deviation of 0.4 A after 30 minutes. During the first half an hour I_d increased up to 2.83 A with sd = 1.0 A before decreasing towards a constant value. The curved anode was able to sustain the thermal load. We did not observe the formation of hot zones.

IV. Conclusion

As demonstrated with the testing of the first wall-less Hall thruster prototype, the performance characteristics are degraded in simple wall-less configuration especially the discharge current and the ionization degree. This study therefore aimed at optimizing the wall-less HT design by adapting the anode geometry and the magnetic field topology. The strategy consists in avoiding the intersection between the anode and the **B** field flux lines in order to prevent short-circuiting of the magnetic barrier. Experiments have been carried out with the 1.5 kW-class PPS-Flex Hall thruster in the CORONA vacuum chamber at EPL and in the PIVOINE-2g test-bench at ICARE. Shaping the anode and adjusting the magnetic field topology in parallel allows to strongly reduce the discharge current, to increase the propellant utilization and to achieve reasonable thrust efficiency. Further optimization is still possible to recover a high efficiency as the maximum B field strength was too low in this work due to the PPS-Flex initial design. A new version of the PPS-Flex able to produce a strong **B** field is presently in development. Moreover, the length of the ceramic cavity could be decreased. This length must however remain long enough to guarantee homogenization of the injected gas. Shortening of the thruster will lead to a decrease in mass and volume.

A Hall thruster in WL configuration would offer significant benefits in terms of integration, operating envelope, lifetime and fuel options. As the thrust is generated outside, the dielectric channel can be considerably shortened, leading to economies in mass and volume. Plasma interaction with the walls will have been significantly reduced. The cavity material will therefore have less influence on the thruster performance, and more importantly, operation at high voltage is presumably possible and lifetime can be extended. Furthermore, reduction in plasma-wall interactions could lead to a large electron temperature, a positive point to allow an efficient ionization of atomic fuels like krypton and argon.

Acknowledgments

This work has been carried out in the frame of the French joint-research program GIS PEE. It was also financially supported by ESA-ESTEC in the frame of the contract #4200021277/07/NL/PA-CCN5. J. Vaudolon benefits from a CNES/Snecma PhD grant. A. Rossi is a Ph.D. candidate with a CNES/Snecma grant.

References

[1] Ahedo E., Plasma for space propulsion, *Plasma Phys. Control. Fusion*, Vol. 53, 2001, 124037

[2] Goebel D. M. and Katz I., Fundamentals of Electric Propulsion, Wiley, Hoboken, 2008, pp. 385-392.

[3] Zhurin V. V., Kaufmann H. R. and Robinson R. S., Physics of closed drift thrusters, *Plasma Sources Sci. Technol.,*Vol. 8, 1999, pp. R1- R20.

[4] Dannenmayer K. and Mazouffre S., Elementary scaling relations for Hall effect thrusters, *J. Propulsion and Power*, Vol. 27, 2011, pp. 236-245.

[5] Mazouffre S., Pérez Luna R. and Dannenmayer K., Examination of plasma-wall interactions in Hall effect thrusters by means of calibrated thermal imaging, *J. Appl. Phys*., Vol. 102, 2007, 023304.

[6] Mazouffre S., Dannenmayer K. and Blank C., Impact of discharge voltage on wall-losses in a Hall thruster, *Phys. Plasmas*, Vol. 18, 2011, 064501.

[7] Mikellides I. G., Katz I., Hofer R. R., Goebel D. M. and deGrys K., Magnetic shielding of the channel walls in a Hall plasma accelerator, Phys. Plasmas, Vol. 18, 2011, 033501.

[8] Mikellides I. G., Katz I., Hofer R. R. and Goebel D. M., Magnetic shielding of walls from the unmagnetized ion beam in a Hall thruster, *Appl. Phys. Lett*., Vol. 102, 2013, 023509.

[9] Mikellides I. G., Katz I., Hofer R. R. and Goebel D. M., Magnetic shielding of a laboratory Hall thruster. I. Theory and validation, *J. Appl. Phys*., Vol. 115, 2014, 043303.

[10] Hofer R. R., Goebel D. M., Mikellides I. G. and Katz I., Magnetic shielding of a laboratory Hall thruster. II. Experiments, *J. Appl. Phys*., Vol. 115, 2014, 043304.

[11] Goebel D. M., Hofer R. R., Mikellides I. G., Katz I., Polk J. E. and Dotson B., Conducting wall Hall thrusters, Proceedings of the 33rd International Electric Propulsion Conference, Washington DC, IEPC paper 13-276, 2013.

[12] Mazouffre S., Vaudolon J., Largeau G., Hénaux C., Rossi A. and Harribey D., Visual evidence of magnetic shielding with the PPS-Flex Hall thruster, *IEEE Trans. Plasma Science*, Vol. 42, 2014, pp. 2668-2669

[13] Mazouffre S., Tsikata S., Vaudolon J., Development and experimental characterization of a wall-less Hall thruster, *J. Appl. Phys.*, Vol. 116, 2014, 243302.

[14] Mazouffre, S. Tsikata S., and Vaudolon J., Development and characterization of a wall-less Hall thruster, Proceedings 50th Joint-Propulsion Conference (Cleveland, Ohio), AIAA Paper 2014–3513 (2014).

[15] Mazouffre S., Bourgeois G., Vaudolon J., Garrigues L., Hénaux C., Harribey D., Vilamot R., Rossi A., Zurbach S., and Le Méhauté D., Development and Testing of Hall Thruster with Flexible Magnetic Field Configuration, J. Propulsion Power, to appear, DOI: 10.2514/1.B35417

[16] Garrigues, L., Mazouffre, S., Hénaux, C., Vilamot, R., Rossi, A., Harribey, D., Bourgeois, G.,Vaudolon, J., and Zurbach, S., Design and first test campaign results with a new flexible magnetic circuit for a Hall Thruster, Proceedings of the 33rd International Electric Propulsion Conference, Paper 2013-250.

[17] Mazouffre S., Bourgeois G., Dannenmayer K. and Lejeune A., Ionization and acceleration processes in a small, variable channel width, permanent magnet Hall thruster, *J. Phys. D: Appl. Physics*, Vol. 45, 2012, 185203.

[18] Lejeune A., Bourgeois G. and Mazouffre S., Kr II and Xe II axial velocity distribution functions in a cross-field ion source, *Phys. Plasmas*, Vol. 19, 2012, 073501.

[19] Mazouffre S., Laser-induced fluorescence diagnostics of the cross-field discharge of Hall thrusters, *Plasma Sources. Sci. Technol.*, Vol. 22, 2013, 013001.

[20] Vaudolon J., Mazouffre S., Indirect determination of the electric field in plasma discharges using laser-induced fluorescence spectroscopy, *Phys. Plasmas*, Vol. 21, 2014, 093505.

[21] Mazouffre S., Bourgeois G., Garrigues L., and Pawelec E., A comprehensive study on the atom flow in the cross-field discharge of a Hall thruster, *J. Phys. D: Appl. Phys*., Vol. 44, 2011, 105203.

[22] Garrigues L, Mazouffre S, Vaudolon J, Tsikata S, Fully Two-Dimensional Particle-In-Cell Monte Carlo Collisions Model of a Wall-Less Hall Thruster, Proceedings of the 34th International Electric Propulsion Conference, IEPC paper 2015-311

[23] Adam J-C., Héron A. and Laval G., Study of stationary plasma thrusters using two-dimensional fully kinetic simulations, *Phys. Plasmas* Vol. 11, 2004, pp. 295-305.

[24] Tsikata S., Lemoine N., Pisarev V. and Grésillon D., Dispersion relations of electron density fluctuations in a Hall thruster plasma observed by collective light scattering, *Phys. Plasmas* Vol. 16, 2009, 033506.

[25] Héron A. and Adam J-C., Anomalous conductivity in Hall thrusters: effects of the non-linear coupling of the electron-cyclotron drift instability with secondary electron emission of the walls, *Phys. Plasmas* Vol. 20, 2013, 082313.

[26] Mazouffre S., Echegut P., Dudeck. M., A calibrated infrared imaging study on the steady state thermal behavior of Hall effect thrusters, *Plasma Sources Sci. Technol.,*Vol. 16, 2007, pp. 13-22

[27] Mazouffre S., Dannenmayer K., and Blank C., Impact of discharge voltage on wall-losses in a Hall thruster, Phys. Plasmas, Vol. 18, 2011, 064501